

Large amplitude oscillation of a polar crown filament in the pre-eruption phase

Hiroaki Isobe^{1,2} and Durgesh Tripathi¹

¹ Department of Applied Mathematics and Theoretical Physics, University of Cambridge, Wilberforce Road, Cambridge CB3 0WA, UK
e-mail: isobe: D.H.Isobe@damtp.cam.ac.uk; tripathi: D.Tripathi@damtp.cam.ac.uk

² Department of Earth and Planetary Science, University of Tokyo, Hongo, Bunkyo-ku, Tokyo 113-0033, Japan
e-mail: isobe@eps.s.u-tokyo.ac.jp

Received 1 February 2006 / accepted 10 February 2006

ABSTRACT

Aims. We report observation of a large-amplitude filament oscillation followed by an eruption. This is used to probe the pre-eruption condition and the trigger mechanism of solar eruptions.

Methods. We used the EUV images from the Extreme-Ultraviolet Imaging Telescope on board SOHO satellite and the H α images from the Flare Monitoring Telescope at Hida Observatory. The observed event is a polar crown filament that erupted on 15 Oct. 2002.

Results. The filament clearly exhibited oscillatory motion in the slow-rising, pre-eruption phase. The amplitude of the oscillation was larger than 20 km s⁻¹, and the motion was predominantly horizontal. The period was about 2 hours and seemed to increase during the oscillation, indicating weakening of restoring force.

Conclusions. Even in the slow-rise phase before the eruption, the filament retained equilibrium and behaved as an oscillator, and the equilibrium is stable to nonlinear perturbation. The transition from such nonlinear stability to either instabilities or a loss of equilibrium that leads to the eruption occurred in the Alfvén time scale (~ 1 hour). This suggests that the onset of the eruption was triggered by a fast magnetic reconnection that stabilized the pre-eruption magnetic configuration, rather than by the slow shearing motion at the photosphere.

Key words. Sun: corona - Sun: coronal mass ejections (CMEs) - Sun: prominences - Sun: filaments

1. Introduction

Filament (prominence) eruptions are associated with various kinds of solar activity, such as coronal mass ejections (CME; Munro et al. 1979; Webb & Hundhausen 1987), flares (Hirayama 1974; Kahler et al. 1988), giant arcade formations (McAllister et al. 1996; Tripathi et al. 2004a; Shiota et al. 2005), and even microflares (Sakajiri et al. 2004). Despite the differences in size, energy and morphology, these eruptive phenomena in the solar atmosphere may be different aspects of a common physical process involving plasma ejection and magnetic reconnection (e.g., Shibata 1999; Priest & Forbes 2002).

Understanding the triggering and driving mechanisms of the solar eruptions is one of the most important issues in current solar physics. Numerous theoretical models have been published on this subject (see review by Forbes 2000). In terms of what actually triggers the onset of eruptions, some involve magnetic reconnection to destabilize the pre-existing magnetic system (e.g., Antiochos et al. 1999; Chen & Shibata 2000; Moore et al. 2001), while others consider either shearing/converging motions at the photosphere (e.g., Mikić &

Linker 1994; Kusano et al. 1995; Priest & Forbes 1995; Török & Kliem 2003) or newly emerging flux with or without reconnection (e.g., Vršnak 1990; Chen & Shibata 2000; Lin et al. 2001; Zhang & Low 2001) that lead to loss of equilibrium or to ideal/resistive instabilities. When investigating which mechanism may be responsible for this onset, several authors studied the morphology, dynamics, associated brightenings, and their relative timing in filament eruptions in detail (e.g., Sterling & Moore 2004, 2005; Williams et al. 2005). The results of these observational studies have not converged yet, and indeed they imply that a combination of several mechanisms may be at work in the same event.

Oscillation of erupting filaments provides an alternative tool for probing the onset mechanisms. Filament oscillation can be classified into two groups (Oliver & Ballester 2002), namely small-amplitude oscillations (velocity $< 2\text{--}3$ km s⁻¹) and large-amplitude ones (velocity ~ 20 km s⁻¹). The large-amplitude oscillations are caused by such flare-related disturbances as Moreton waves (Ramsey & Smith 1966; Eto et al. 2002), EIT waves (waves observed by the Extreme-Ultraviolet Imaging Telescope on SOHO, Okamoto et al. 2004), and nearby microflares (Jing et al. 2003). Observations

of such large-amplitude oscillations can be used to examine the physical parameters and the equilibrium properties of filaments (Hyder 1966; Kleczek & Kuperus 1969; Vrřnak 1984). However, the number of reported observations of large-amplitude oscillations is still small. Moreover, most of them are of quiescent filaments, while there are few observations of the oscillation of active filaments (Vrřnak et al. 1990).

In this letter we report the observation of a large-amplitude oscillation and the subsequent eruption of a polar crown filament. The oscillation occurred after the filament started to rise slowly, and sudden acceleration and eruption followed the oscillation. We examine the motion and amplitude of the oscillation and discuss what it indicates about the onset mechanism of the eruption.

2. Observation

The oscillation and subsequent eruption of a filament was found while the authors were searching for the filament eruption events in the list of EUV post-eruptive arcades published by Tripathi et al. (2004b). The filament is a large polar crown that erupted on 15 Oct. 2002. A CME was observed following the eruption, but no flare was recognized in the GOES light curve. In this study we mainly use the 195 Å images from the Extreme-Ultraviolet Imaging Telescope (EIT; Delaboudinière et al. 1995) on the *Solar and Heliospheric Observatory* (SOHO). The time cadence of 195 Å images is about 12 minutes, and the spatial resolution is 2.6 arcsec.

The filament was also observed by the Flare Monitoring Telescope (FMT; Kurokawa et al. 1995) at Hida Observatory, Kyoto University. The FMT observes the full disk of the Sun in 5 channels including H α line centre and wings at ± 0.8 Å with a time cadence of 2 s and a spatial resolution of 4.25 arcsec. Unfortunately, due to frequent interruption by clouds, the oscillatory motion is not clear, and the eruption occurred during the night at Hida observatory. However, the H α ± 0.8 Å images provide useful information on the line-of-sight motion of the filament.

3. Results

Figure 1 shows the EIT 195 Å images of the filament, in its pre-eruption and eruption phases. The filament has an arch-like shape in the pre-eruption phase, with the ends near (-100, -500) and (-700, -600) in the solar disk coordinate system. The oscillatory motion was seen only in a part of the filament indicated by the box in Fig. 1.

To illustrate the motion of filament, Fig. 2 shows the intensity evolution along the slits 1 and 2 in Fig. 1 (time slices), corrected for solar rotation. The time slice for slit 1 shows that the filament was slowly rising for more than 10 hours until it was suddenly accelerated at around 11:30 UT followed by the eruption. The rising velocity of this pre-eruption phase is about 1 km s^{-1} . The oscillatory motion is not evident at the position of slit 1. On the other hand, the time slice for slit 2 clearly shows the oscillation, as well as the general trend to slow rising. The oscillation started at about 02:50 UT and was repeated three times before the filament finally erupted. The existence of

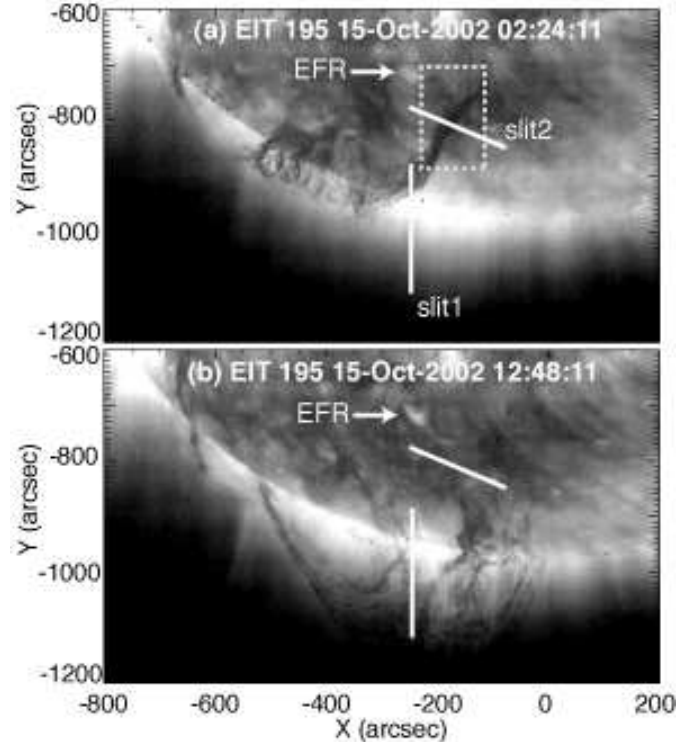


Fig. 1. EIT images of the erupting filament: (a) pre-eruption phase and (b) eruption phase. The solid lines indicate the slit positions of time slices shown in Fig. 2. The dashed-line box shows the field of view of Fig. 3. The arrow points to the emerging flux region (EFR) near the filament.

the fourth oscillation is not clear because the eruption (strong acceleration) started after the third oscillation. As indicated in Fig. 2, the velocity of the oscillation was about $4\text{-}5 \text{ km s}^{-1}$, and the amplitude of displacement was about 20-30 arcsecs (not indicated in the figure). Note that the velocities and displacements are measured on the plane of the sky.

We did not find any flares or microflares at the onset of the oscillation. It was possibly triggered by the emerging flux under the oscillating part of the filament, which is indicated in Fig.1. The emerging flux was first identified as a growing bipolar region in magnetograms from the Michelson Doppler Imager aboard SOHO at 19:15 UT on 14 Oct. 2002. As a coronal counterpart, this growing bipole was seen as bright loops in the EIT images. Emerging fluxes often undergo reconnection with a pre-existing coronal field to produce small flares and jets (e.g., Isobe et al. 2005). However, the intensity of the emerging flux in EIT images did not increase for several hours before and after the onset of oscillation. Probably the reconnection did occur and excited the oscillation, but the plasma heating and/or chromospheric evaporation were too weak to increase the coronal EUV emission, due to the weak magnetic field in this region (Yamamoto et al. 2002; Vrřnak & Skender 2005).

The vertical white lines in Fig. 2 indicate the times at which the direction of the oscillating motion seems to reverse. The reversal points are not clear from the time slices, particularly for the fourth oscillation where the eruption started. If we assume that the white lines in Fig.2 give the correct reversal

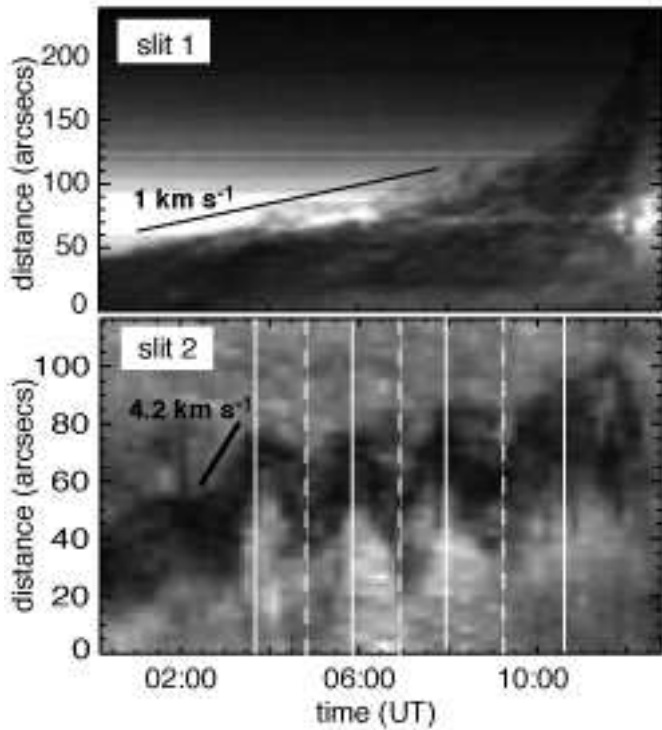


Fig. 2. Time slices for slit 1 (upper panel) and slit 2 (lower panel). The positions of the slits are indicated in Fig. 1. The distance is measured from the northern end of each slit. The black solid lines show the velocity of the filament along the slits. The vertical white lines in the lower panel indicate the reversal points of the oscillation; the solid and dashed lines correspond to the opposite phases.

points, the period of the oscillation increases slightly from 2 hours to 2.6 hours. This indicates the weakening of the restoring force, which may also be related to the destabilization and onset of the filament eruption. However, considering the uncertainty of the reversal points due to the internal structure of the filament and the course cadence (12 min) of EIT data, we hesitate to make any conclusive suggestions about the period increase based only on these data.

The three-dimensional motion of the filament can be probed by combining the motions in the images and the information of Doppler shift. Figure 3 shows the images of the blue wing (-0.8\AA ; panels a and c) and the red wing ($+0.8\text{\AA}$; panels b and d) of $H\alpha$ taken by FMT at 04:12 UT and 05:27 UT. The field of view is the same as the box in Fig. 1. The overlaid contours show the EIT intensity extracted from the EIT images recorded at the nearest times. The contour level is $40 \text{ DN s}^{-1} \text{ pix}^{-1}$, tracing the darkest part of the filament where the oscillation is evident.¹ The arrows show the velocity field on the plain of the sky calculated by correlation tracking. The velocity field shows that the oscillatory motion is predominantly perpendicular to the filament axis. Also, the phase of the oscillation is nearly the same along the filament, i.e., the oscillating part of the filament moves like a rigid body. The other parts of

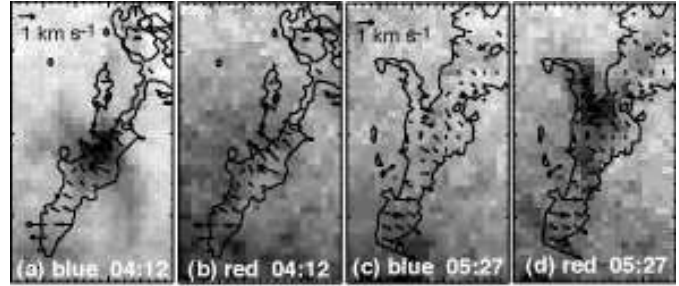


Fig. 3. $H\alpha$ wing images at 04:12 UT (panels a and b) and at 05:27 UT (panels c and d). Panels a and c are of the blue wing at -0.8\AA and panels b and d are of the red wing at $+0.8 \text{\AA}$. Overlaid are $40 \text{ DN s}^{-1} \text{ pix}^{-1}$ contour at 04:12 UT (panels a and b) and at 05:24 UT (panels c and d). The arrows show the velocity field on the plane of the sky calculated by correlation tracking of the EIT images. The velocity field is shown only in the region where the EIT count is less than $40 \text{ DN s}^{-1} \text{ pix}^{-1}$.

the filament, those outside the box in Fig. 1, do not exhibit any oscillatory motion.

At 04:12 UT (panels a and b) the filament is seen as a dark feature in the blue wing, whereas it is almost invisible in the red wing. Thus it is moving towards the observer. The motion on the plane of sky is northeastward at this time. At 05:27 UT (panels c and d) when the motion on the plane of sky becomes southwestward, the filament appears in the red wing and disappears in the blue wing. This is the well-known feature of the “winking filament” (Hyder 1966; Okamoto et al. 2004).

Morimoto & Kurokawa (2003) have developed a method to determine the line-of-sight velocity from the contrasts of $H\alpha$ wing images, and applied the method to 5 filament eruptions observed by the FMT. In this event the intensity of the darkest region in blue wing image is about 35 % less than the surrounding region at 04:12 UT. If we assume that the physical parameters of the filament such as the source function, optical depth, and line width are similar to those of the filaments analysed by Morimoto & Kurokawa (2003), the contrast of 35 % in the FMT blue wing corresponds to the line-of-sight velocity of $20\text{--}30 \text{ km s}^{-1}$, which is several times larger than the velocity on the plane of sky.

Since the filament was located near the southern limb, the above results indicate that the oscillatory motion is predominantly horizontal (Kleczeck & Kuperus 1969). If the motion is purely vertical, the blue and red shifts of $H\alpha$ should be accompanied by a southward and northward motion, respectively, whereas the data show the blue shift with the northeastward motion and the red shift with the southwestward motion. This is consistent with the predominantly horizontal motion.

According to the model by Kleczeck & Kuperus (1969), the period P of the horizontal oscillation of a filament is given by $P = 4\pi LB^{-1} \sqrt{\pi\rho}$, where $2L$ is the length of the oscillating filament, ρ the mass density, and B the strength of the effective magnetic field that causes the restoring force of the oscillation; namely the period is of the order of the Alfvén transit time of the filament. Assuming $\rho = 10^{-13} \text{ g cm}^{-3}$, B and the Alfvén velocity $V_A = B / \sqrt{4\pi\rho}$ can be calculated from the measured

¹ see Delaboudinière et al. (1995) for the definition of DN.

values of $L = 10^{10}$ cm and $P = 7200$ s; $B = 1.4$ Gauss and $V_A = 12$ km s⁻¹. These are reasonable values considering that the filament is located in the polar region where the magnetic field is weak.

4. Discussion

A slow rise in the pre-eruption phase and the subsequent sudden acceleration and eruption are commonly observed not only in filament eruptions but also in X-ray plasmoid ejections and coronal mass ejections (Ohyama & Shibata 1997; Zhang et al. 2001; Sterling and Moore 2005). The large amplitude of the oscillation reported in this letter suggests that, even during the slowly rising phase, the filament still retains the equilibrium, and furthermore the equilibrium is *nonlinearly* stable. Thus the slow rise in the pre-eruption phase is a quasi-static evolution, rather than the very slow linear stage of instability.

Furthermore, the time scale of the transition from such nonlinearly stable equilibrium to the fast eruption by instability or loss of equilibrium was quite short, at most the Alfvén transit time of the filament (~ 1 hour). This suggests that the fast eruption was triggered by the fast magnetic reconnection that changes the equilibrium property of the magnetic system, rather than by the slow shearing/converging motions at the photosphere. However, the energy accumulation and slow rise may be driven by the photospheric motions. Such destabilizing reconnection can occur either at the overlying arcade above the filament (Antiochos et al. 1999) or near the footpoint (Chen & Shibata 2000; Moore et al. 2001; Tripathi 2005). The emerging flux may also trigger the eruption without reconnection (Vršnak 1990; Lin et al. 2001). However, we did not find significant increase in the magnetic flux in the emerging flux region at the time of eruption onset, so probably it cannot explain the fast transition from oscillation to eruption observed in this event. We should note that in this event only a part of the filament exhibited the oscillation, so the equilibrium properties of the whole filament system may not be nonlinearly stable during the observed oscillation. Further search for such an oscillation of erupting filaments is desirable.

The increase in the oscillation period, though not conclusive, indicates that the restoring force became weak during the oscillation. Hence, it may correspond to the destabilizing process for the eruption, and may be consistent with the destabilizing reconnection as the triggering mechanism. It is interesting to see whether current analytical and numerical models of erupting filaments can oscillate with large amplitude and, if so, how the filament's properties as an oscillator change with time before and at the onset of the eruption.

Acknowledgements. The authors thank M. Kadota, H. Komori, and T. Okamoto for their help in preparing and analysing the FMT data, and H. E. Mason for useful comments. HI is supported by the Research Fellowship from the Japan Society for the Promotion of Science for Young Scientists. DT acknowledges funding from PPARC. SOHO is a project of international collaboration of ESA and NASA. Moreover, we would also like to acknowledge Castle, a pub in Cambridge, where the idea of this paper first came up and was developed.

References

- Antiochos, S. K., DeVore, C. R., & Klimchuk, J. A. 1999, *ApJ*, 510, 485
- Chen, P. F., & Shibata, K. 2000, *ApJ*, 545, 524
- Delaboudinière, J. P., Artzner, G. E., Brunaud, J. et al. 1995, *Sol. Phys.*, 162, 291
- Eto, S., Isobe, H., Narukage, N. et al. 2002, *PASJ*, 54, 481
- Forbes, T. G. 2000, *J. Geophys. Res.*, 105, 23153
- Hirayama, T. 1974, *Sol. Phys.*, 34, 323
- Hyder, C. L. 1969, *ZAp*, 63, 78
- Isobe, H., Miyagoshi, T., Shibata, K., & Yokoyama, T. 2005, *Nature*, 434, 478
- Jing, J., Lee, J., Spirock, T. J. et al. 2003, *ApJ*, 584, L103
- Kleczek, J., & Kuperus, M. 1969, *Sol. Phys.*, 6, 72
- Kahler, S. W., Moore, R. L., Kane, S. R., & Zirin, H. *ApJ*, 328, 824
- Kurokawa, H., Ishiura, K., Kimura, G. et al. 1995, *Geoelectr.*, 47, 1043
- Kusano, K., Suzuki, Y., & Nishikawa, K. 1995, *ApJ*, 441, 942
- Lin, J., Forbes, T. G., Isenberg, P. A. 2001, *J. Geophys. Res.*, 106, 25,053
- McAllister, A. H., Dryer, M., McIntosh, P., Singer, H., & Weiss, L. 1996, *J. Geophys. Res.*, 101, 13497
- Mikić, Z., & Linker, J. A. 1994, *ApJ*, 430, 898
- Moore, R. L., Sterling, A. C., Hudson, H. S., & Lemen, J. R. 2001, *ApJ*, 552, 833
- Morimoto, T., & Kurokawa, H., 2003, *PASJ*, 55, 503
- Munro, R. H., Gosling, J. T., Hildner, E. 1979, *Sol. Phys.*, 61, 201
- Ohyama, M., & Shibata, K. 1997, *PASJ*, 49, 249
- Okamoto, T.J., Nakai, H., Keiyama, A. et al. 2004, *ApJ*, 608, 1124
- Oliver, R., & Ballester, J. L. 2002, *Sol. Phys.*, 206, 45
- Priest, E. R., & Forbes, T. G. 1995, *ApJ*, 446, 377
- Priest, E. R., & Forbes, T. G. 2002, *A&A Rev.*, 10, 313
- Ramsey, H., & Smith, S. F. 1966, *AJ*, 71, 197
- Sakajiri, T., Brooks, D. H., Yamamoto, T., et al. 2004, *ApJ*, 616, 578
- Shiota, D., Isobe, H., Chen, P. F., et al. 2005, *ApJ*, 634, 663
- Shibata, K. 1999, *Ap&SS*, 264, 129
- Sterling, A. C., & Moore, R. L. 2004, *ApJ*, 602, 1024
- Sterling, A. C., & Moore, R. L. 2005, *ApJ*, 630, 1148
- Török, T. & Kliem, B. 2003, *A&A*, 406, 1043
- Tripathi, D. 2005, Ph.D. thesis, University of Göttingen, Copernicus, GMBH
- Tripathi, D., Bothmer, V., & Cremades, H. 2004a, *A&A*, 422, 337
- Tripathi, D., Bothmer, V., & Cremades, H. 2004b, *yCat*, 34220337T
- Vršnak, B. 1984, *Sol. Phys.*, 94, 289
- Vršnak, B. 1990, *Sol. Phys.*, 129, 295
- Vršnak, B., & Skender, M. 2005, *Sol. Phys.*, 226, 97
- Vršnak, B., Ruždjak, V., Brajša, R. & Zloch, F. 1990, *Sol. Phys.*, 127, 119
- Webb, D. F., & Hundhausen, A. J. 1987, *Sol. Phys.*, 108, 383
- Williams, D. R., Török, T., Démoulin, P., van Driel-Gesztelyi, L., & Kliem, B. 2005, *ApJ*, 628, L163
- Yamamoto, T. T., Shiota, D., Sakajiri, T. et al. 2002, *ApJ*, 579, L45
- Zhang, J., Dere, K. P., Howard, R. A., Kundu, M. R., & White, S. M. 2001, *ApJ*, 559, 452
- Zhang, M., & Low, B. C. 2001, *ApJ*, 561, 406